On the Cyclability of the Thermochromism in $CuMoO_4$ and Its Tungsten Derivatives $CuMo_{1-x}W_xO_4$ ($x < 0.12$)

Anne-Emmanuelle Thiry,[†] Manuel Gaudon,*[,‡] Christophe Payen,[†] Nathalie Daro,[‡] Jean-François Létard,[‡] Stéphane Gorsse,[‡] Philippe Deniard,[†] Xavier Rocquefelte,[†] Alain Demourgues,[‡] Myung-Hwan Whangbo,*[,§] and Stéphane Jobic*[,†]

Institut des Matériaux Jean Rouxel, UMR 6502 CNRS-Université de Nantes, 2 rue de la Houssinière, BP 32229, 44322 Nantes, France, Institut de Chimie de la Matière Condensée de Bordeaux, UPR 9048 CNRS 87 avenue du Dr. Schweitzer, 33608 Pessac Cedex, France, and Department of Chemistry, North Carolina State University, Raleigh, North Carolina 27695-8204

Received January 3, 2008
Revised Manuscript Received February 1, 2008

A thermochromic substance changes its color when subjected to a temperature variation in a certain range. For practical reasons, the thermochromism should occur in the temperature range appropriate for desired applications. $CuMoO_4$ exhibits thermochromism[1–3] in the temperature region between ~175 and ~260 K, which depends strongly on the heating/cooling rate, and has two polymorphs, that is, the high temperature (HT) form (i.e., α form) and the low temperature (LT) form (i.e., γ form). The temperature-induced color change in $CuMoO_4$ originates from a first order phase transition between the two structures (with ~10% shrinking of the unit cell volume at the transition).[4] A recent study of tungsten-doped derivatives of $CuMoO_4$, that is, $CuMo_{1-x}W_xO_4$ ($x < 0.12$), showed that the temperature range of their thermochromism can be raised to a more easily accessible range.[5,6] These materials are thus attractive for uses around room temperature. For example, at ambient pressure, $CuMo_{0.9}W_{0.1}O_4$ changes its color from red to green by warming above ~360 K and from green to red by cooling below ~275 K. Furthermore, the color change from green to red can be triggered by applying a weak pressure (e.g., finger push; Figure S1 of the Supporting Information), and the green color is regained by heating.[5,6] The α- and γ-type structures of $CuMoO_4$ are maintained in the $CuMo_{1-x}W_xO_4$ ($x < 0.12$) solid solution. It is of interest to probe how well $CuMoO_4$ and its tungsten derivatives can withstand repeated cooling/warming (C/W) cycles without losing their thermochromism significantly. In the present work we examine this question of cyclability by performing optical absorbance (OA) at 520 nm, differential scanning calorimetry (DSC) analyses, and magnetic susceptibility measurements as well as spin dimer analysis for the α and γ structures of $CuMoO_4$. Our study reveals that, after a number of repeated cooling/warming cycles, the α-form loses its ability to transform into the γ-form. The structural and physical properties of $CuMo_{1-x}W_xO_4$ ($x < 0.12$) are not reported here because of their strong similarities to those of $CuMoO_4$.

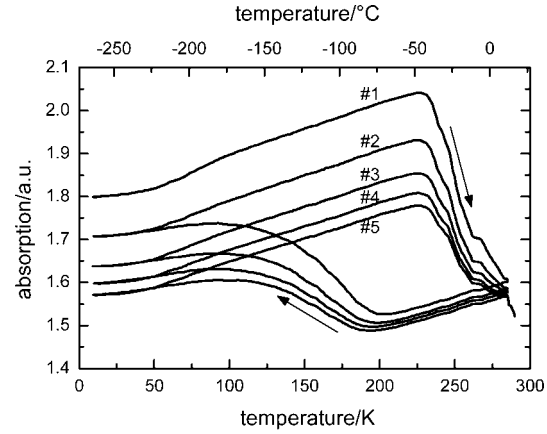

Figure 1. Evolution of the OA at 520 nm of $CuMoO_4$ vs temperature and upon cycling with a cooling/warming rate of 1.5 $K \cdot min^{-1}$. The arrows indicate the cooling/warming curves.

Figure 1 shows how the OA value at 520 nm of $CuMoO_4$ varies during the C/W cycles between 10 and 300 K with C/W rate of 1.5 $K \cdot min^{-1}$ (see Figure S2 of the Supporting Information for measurements with a 5 $K \cdot min^{-1}$ C/W rate). At high temperature, the single phase material is green so that the light of wavelength 520 nm is reflected hence falling down the OA values. When the temperature is lowered, the green to red transition occurs. Thus, the reflectivity spectrum changes with absorption ranging approximately from orange to UV, and the OA value increases.[5,6] To a first approximation, the OA value at 520 nm reflects the relative percentage of the α and γ forms in the probed sample. Once the α → γ transition is initiated by cooling, the α form can be recovered by warming. However, at the second cooling, only a part of the α form changes to the γ form. With increasing the number of C/W cycles, the amount of the α form that changes to the γ form decreases progressively so that the hysteresis loop of the OA versus T plot progressively becomes smoothed out, and finally the α form is stabilized in a wider temperature range. Experiments carried out with different C/W rates lead to the same observations except that, at a lower C/W rate, the total disappearance of the γ-form requires more C/W cycles without change in the transition temperatures.

Figure 2 gives the evolution of the heat flow on heating at 20 $K \cdot min^{-1}$ between 200 K and 453 K observed for

* Corresponding author. E-mail: stephane.jobic@cnrs-imn.fr (S.J.); mike_whangbo@ncsu.edu (M.-H.W.), gaudon@icmcb-bordeaux.cnrs.fr (M.G.).
[†] Institut des Matériaux Jean Rouxel.
[‡] Institut de Chimie de la Matière Condensée de Bordeaux.
[§] North Carolina State University.

(1) Hernández, D.; Rodríguez, F.; Garcia-Jaca, J.; Ehrenberg, H.; Weitzel, H. *Phys. B* **1999**, *265*, 181.
(2) Hernández, D.; Rodríguez, F. *Phys. Rev. B* **2000**, *61*, 16497.
(3) Steiner, G.; Salzer, R.; Reichelt, W. *Fresenius' J. Anal. Chem.* **2001**, *370*, 731.
(4) Ehrenberg, H.; Weitzel, H.; Paulus, H.; Wiesmann, M.; Wltschek, G.; Geselle, M.; Fuess, H. *J. Phys. Chem. Solids* **1997**, *58*, 153.
(5) Gaudon, M.; Deniard, P.; Demourgues, A.; Thiry, A.-E.; Carbonera, C.; Le Nestour, A.; Largeteau, A.; Létard, J.-F.; Jobic, S. *Adv. Mater.* **2007**, *19*, 3517.
(6) Gaudon, M.; Carbonera, C.; Thiry, A.-E.; Demourgues, A.; Deniard, P.; Payen, C.; Létard, J.-F.; Jobic, S. *Inorg. Chem.* **2007**, *46*, 10200.

10.1021/cm703600g CCC: $40.75
Published on Web 02/23/2008

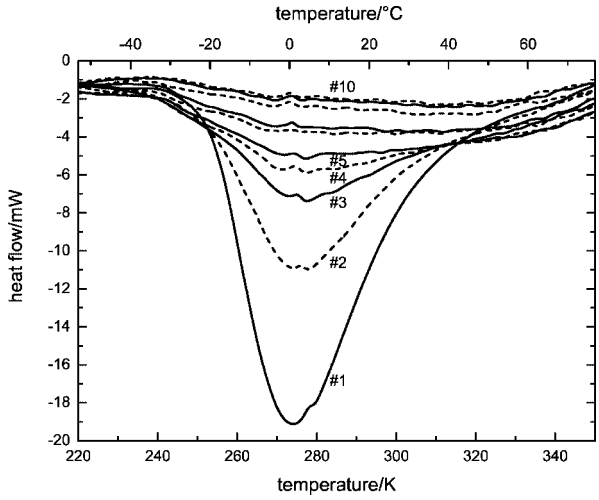

Figure 2. Evolution of the DSC curve of $CuMoO_4$ on warming cycle.

$CuMoO_4$ for the first 10 C/W cycles. The enthalpy change associated with the $\gamma \rightarrow \alpha$ transition at about 272 K is estimated to be $+6.84\ J \cdot g^{-1}$ ($1.53\ kJ \cdot mol^{-1}$) in the first cycle, falls down to $+0.7\ J \cdot g^{-1}$ ($0.16\ kJ \cdot mol^{-1}$) after six cycles, and approaches zero thereafter. Similar trends are found for $CuMo_{0.9}W_{0.1}O_4$; the enthalpy change is $+12.14\ J \cdot g^{-1}$ (2.82 $kJ \cdot mol^{-1}$) in the first cycle and decreases to $+2.71\ J \cdot g^{-1}$ ($0.63\ kJ \cdot mol^{-1}$) after 10 cycles. Data collected on cooling gave rise to a broad and diffuse exothermic peak, which is difficult to analyze. Nevertheless, the peak intensity decreases with increasing the number of C/W cycles. Thus, results of DSC measurements are consistent with the conclusion from the OA measurements that the HT-form loses its ability to transform into the LT-form progressively as the number of C/W cycles increases.

We now examine the cyclability of the thermochromism in $CuMoO_4$ on the basis of magnetic susceptibility measurements. The $1/\chi$ versus T plot measured for the first C/W cycle (with $2\ K \cdot min^{-1}$) is shown in Figure 3a. On cooling the sample from 300 K to 200 K, the susceptibility of the α form follows a Curie–Weiss law, $\chi(T) = C_\alpha/(T - \theta_\alpha)$ with $\theta_\alpha \approx -19$ K and $C_\alpha \approx 0.46\ cm^3\ K\ mol^{-1}$. The latter C_α value leads to the effective moment of 1.87 μ_B per Cu atom, which is consistent with Cu^{2+} ($S = 1/2$) and $g \approx 2.2$. At lower temperatures, the $\alpha \rightarrow \gamma$ transition induces a deviation from the high-temperature Curie–Weiss behavior. As can be seen from the χT versus T plot (Figure 3b), a rapid decrease of χT begins at about 190 K on cooling, and a new low-temperature Curie–Weiss regime is observed below about 100 K. Because the $\alpha \rightarrow \gamma$ transition does not change the +2 oxidation state of Cu, the decrease in χT between 190 and 100 K indicates the occurrence of strong antiferromagnetic (AFM) spin exchange interactions that couple some Cu spins into units with diamagnetic singlet state in the low temperature γ phase (for further discussion, see below). Between 80 and 10 K, a Curie–Weiss fit leads to $\theta_{LT} \approx -5$ K and $C_{LT} \approx 0.25\ cm^3\ K\ mol^{-1}$. Both the negative θ_{LT} and the decrease in χT between 100 and 5 K suggest that weak AFM interactions occur between the remaining spins not involved in the formation of the diamagnetic units. There is no evidence for a long-range magnetic ordering in the

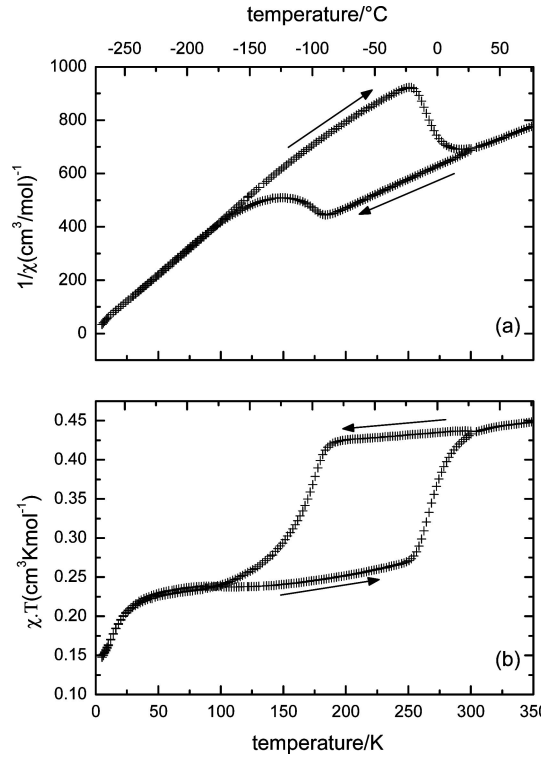

Figure 3. Temperature dependence of (a) $1/\chi$ and (b) χT of $CuMoO_4$. The arrows indicate the cooling and warming curves.

investigated temperature range. On warming, a pronounced hysteresis effect is observed in the 190−250 K region, which is consistent with a first-order transition. Figure 4a presents the χT vs T curves observed for $CuMoO_4$ for a number of successive C/W cycles. The variations of χT at 190 K (on cooling) and 250 K (on warming) are less and less pronounced when the number of C/W cycles increases. The Curie constants, extracted from the Curie–Weiss fits for the HT (200–280 K) and LT (20–80 K) regions, are plotted as a function of the cycle sequence (see Figure 4b). With increasing the number of cycles, the HT Curie constant remains nearly constant but the LT Curie constant increases significantly. To gain insight into the magnetic properties of $CuMo_{1-x}W_xO_4$, we evaluate the spin exchange interactions in the α and γ structures of $CuMoO_4$ by performing spin dimer analysis based on extended Hückel tight binding (EHTB) calculations.[7] As summarized in Figures S3 and S4 of the Supporting Information, there are nine spin exchange paths to examine in the α form, and seven spin exchange paths in the γ form. The strength of a spin exchange interaction between two spin sites is described by a spin exchange parameter $J = J_F + J_{AF}$, where J_F is the ferromagnetic term ($J_F > 0$) and J_{AF} is the antiferromagnetic term ($J_{AF} < 0$). In most cases J_F is very small so that the trends in the J values are well approximated by those in the corresponding J_{AF} values. For a spin dimer in which each spin site contains one unpaired spin, the J_{AF} term is approximated by $J_{AF} \approx -(\Delta\varepsilon)^2/U_{eff}$ where U_{eff} is the effective on-site repulsion, which is essentially a constant for a given compound. If the

(7) Whangbo, M.-H.; Koo, H.-J.; Dai, D. *J. Solid State Chem.* **2003**, *176*, 417. Whangbo, M.-H.; Dai, D.; Koo, H.-J. *Solid State Sci.* **2005**, *7*, 827.

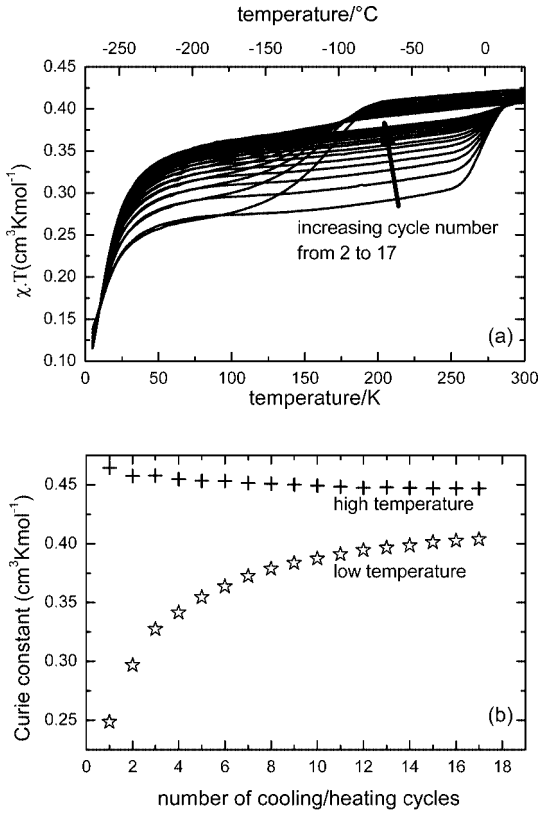

Figure 4. (a) Temperature dependence of χT for $CuMoO_4$ as a function of the C/W cycles. (b) Evolution of the Curie constants of $CuMoO_4$ for the high-temperature (200−280 K) and the low-temperature (20−80 K) regions as a function of the C/W cycles.

two spin sites are equivalent, $\Delta\varepsilon$ is the energy difference Δe between the two magnetic orbitals representing the spin dimer. When the two spin sites are nonequivalent, $(\Delta\varepsilon)^2 = (\Delta e)^2 - (\Delta e^0)^2$, where Δe^0 is the energy difference between the magnetic orbitals representing each spin site of the spin dimer ($\Delta e^0 = 0$ if the two spin sites are equivalent). In the present work, the Δe and Δe^0 values for various spin dimers are evaluated by performing EHTB calculations (Table S1, Supporting Information). Results of our spin dimer analysis are summarized in Table S2 (Supporting Information). In the α form, all spin exchange interactions are weak, which is consistent with the effective paramagnetic moment and the small $\theta_\alpha \approx -19$ K observed in the first cooling cycle. In the γ form, there is a very strong AFM spin exchange interaction associated with each nearly linear Cu(2)–O−Cu(3) superexchange path and all other spin interactions are weak. A rough estimation of the strongest Cu(2)–O−Cu(3) superexchange interaction J can be done by comparison with other copper oxides. Namely, in layered and one-dimensional cuprates for which the relevant Cu–O–Cu bond angle equals 180°, the nearest-neighbor interaction $|J|$ lies in the range 1200–2300 K.[8] The value of $|J|$ decreases as the bond angle deviates from 180° and the Cu–O distance increases. In $BaCu_2Ge_2O_7$,[9] for instance, a value of $|J| \approx 540$ K is associated with a bond angle of 135° and a Cu–O distance of 1.97 Å. In γ-$CuMoO_4$, the Cu(2)–O−Cu(3) bond angle of 150° and the short Cu–O distance of about 1.91 Å will thus lead to a $|J|$ value much higher than 540 K (of the order of 1000 K). Such a strong AFM interaction between the Cu(2) and Cu(3) sites form isolated AFM dimers giving rise to a very small contribution to the low temperature magnetic susceptibility, and the Cu(1) spins become isolated and hence become paramagnetic. Because there are equal numbers of the Cu(1), Cu(2), and Cu(3) sites, the Curie constant in the low-temperature region should be reduced by a factor of 3 from that in the high temperature region if the α form is completely converted to the γ form on cooling. For the first cooling cycle, the observed $C_{LT} \approx 0.25$ cm^3 K mol^{-1} is higher than the expected value $C_\alpha/3 \approx 0.15$ cm^3 K mol^{-1}. Therefore, the increase in the low-temperature Curie constant, shown in Figure 4b, indicates that the conversion of the α form to the γ form becomes less efficient with increasing the number of C/W cycles. This agrees with the conclusion reached from the OA and DSC measurements, and is also consistent with in situ diffraction experiments from 240 to 130 K,[4] which evidenced that a single phase α-$CuMoO_4$ sample is partially transformed into a γ-$CuMoO_4$ upon cooling, with the residual pristine high temperature form estimated to be more than 10%.

It appears important to consider why the α-form progressively loses its ability to become the γ-form as the number of C/W cycles increases. Two hypotheses may be envisaged. First, crystal growth is hindered with increasing the number of C/W cycles because the size of crystallites becomes smaller than a critical size. Namely, the $\alpha \rightleftarrows \gamma$ transformation involves about 10% change in the unit cell volume, which triggers crack formation within crystals so that crystallites become progressively smaller in size as the number of C/W cycles increases. However, this hypothesis seems inconsistent with the observation that the cyclability of $CuMoO_4$ is better when the C/W rate is faster (see Figure S2 of the Supporting Information). Moreover, XRD analyses on $CuMoO_4$ before and after 17 C/W cycles show no change in the coherence lengths ξ of α-$CuMoO_4$, that is, $\xi > 200$ nm (with no trace of residual γ-$CuMoO_4$) even if SEM analyses reveal the anisotropy of the grains after several C/W cycles becomes more noticeable and crystals larger than 20 μm disappear. Second, the successive $\alpha \rightleftarrows \gamma$ pseudo-reconstructive/diffusionless transitions might generate defects that favor the stabilization of the HT form at the expense of the LT form upon cycling.

Supporting Information Available: Experimental section, Figures S1, S2, S3 and S4, and Tables S1 and S2 (PDF). This material is available free of charge via the Internet at http://pubs.acs.org.

CM703600G

(8) Mizuno, Y.; Tohyama, T.; Maekawa, S. *Phys. Rev. B* **1998**, *58*, R14713.

(9) Tsukada, I.; Sasago, Y.; Uchinokura, K.; Zheludev, A.; Maslow, S.; Shirane, G.; Kakurai, K.; Ressouche, E. *Phys. Rev. B* **1999**, *60*, 6601.